Supporting Information

Infrared Photo-Activation Reduces Peptide Folding and H-Atom Migration Following ETD Tandem Mass Spectrometry

Aaron R. Ledvina, Graeme C. McAlister, Myles W. Gardener, Suncerae I. Smith, James A. Madsen, Jennifer S. Brodbelt, and Joshua J. Coon*

Expanded Dataset:

peptide	charge state	precursor m/z	fold-increase in product TIC	ETD sequence coverage	AI-ETD sequence coverage	% sequence coverage increase
KAAAKAAAK	2	415	1.3	*100%*	*100%*	0%
DRVYIHPFL	3	433	1.1	*89%*	*89%*	0%
RPKPQQFFGLM	3	450	1.6	*80%*	*80%*	0%
FSWGAEGQR	2	519	2.1	75%	*100%*	25%
AGCKNFFWKTFTSC	3	546	1.9	54%	92%	38%
SYSMEHFRWGKPV-GKKRRPVKVYP	5	587	1.3	70%	*87%*	17%
DRVYIHPFL	2	648	1.3	44%	56%	12%
RPKPQQFFGLM	2	675	2.7	50%	*80%*	30%
SYSMEHFRWGKPV-GKKRRPVKVYP	4	734	1.9	52%	83%	31%
AGCKNFFWKTFTSC	2	820	2.6	15%	85%	70%
SYSMEHFRWGKPV-GKKRRPVKVYP	3	978	2.2	13%	70%	57%
AVERAGE			1.8	58%	84%	26%

Supporting Information Figure S1. Summary of peptide sequence coverage for ETD and AI-ETD. Italicized, red numbers indicate the maximum possible ETD sequence coverage when considering that cleavage N-terminal to proline is forbidden. Total Ion Current (TIC) was calculated for ETD and AI-ETD by subtracting unreacted precursor and charge reduced regions from the overall TIC associated with a given spectrum.

Effect of Laser Intensity:

Supporting Figure 2 displays the effect of laser power on product ion formation during AI-ETD. As power is increased from 50 to 99% (50W max) so does the intensity of the $z_7^{\bullet}$*-type* product ion. A simultaneous reduction in the H atom transfer product (*i.e.*, *z-type*) is likewise observed, consistent with previous AI-ECD studies.[1] Due to the relatively high pressure of the system (~ 3 mTorr) IR activation did not induce detectable *b-*, *w-*, or *y-type* fragment formation, even at the highest laser power settings.

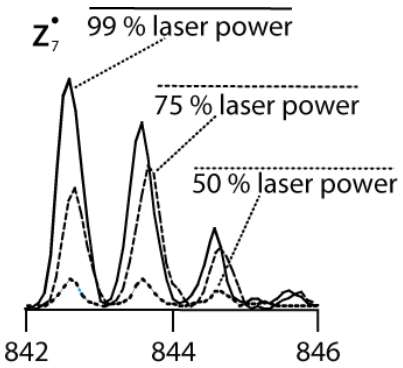

Supporting Information Figure S2. The distribution/intensity of the $z_7^{\bullet}$ product ion generated from a 100 ms AI-ETD reaction of ACTH at various laser powers.

AI-ETD of ubiquitin ions:

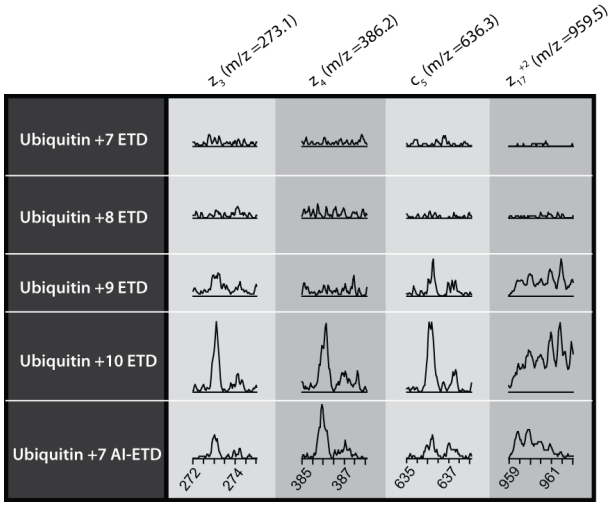

Supporting Information Figure 3. Selected product ion following either ETD or AI-ETD of various precursor charge states of ubiquitin. Product ions z_3, z_4, c_5, and z_{17}^{+2} for ETD of +7 through +10 charge states and +7 AI-ETD. Results shown represent the average of approximately 150 spectra. Note that AI-ETD leads to the formation of product ions that are only upon following ETD of higher charge states. Note y-axis scale is ion intensity (arbitrary units) and is fixed for all spectra.

Shown in Supporting Figure 3 are the $z^{\bullet}_3$, $z^{\bullet}_4$, c_5, and $z^{\bullet}_{17}{}^{+2}$ ETD product ions for the +7 through +10 ubiquitin precursors and the AI-ETD reaction with the +7 precursor. Clemmer et al. have studied ubiquitin conformations under similar pressures using an ion trap/ion mobility mass spectrometry system.[12] Their work revealed the +7 charge state to be in a compact conformation (cross section ~ 1000 $Å^2$) during the time-scale of our experiments (i.e., 10 ms). As charge state increases, so does the cross-section so that the +10 precursor is described as elongated (~ 1500 $Å^2$). Direct ETD of + 7 precursors produced no detectable fragmentation, low level dissociation was detected for the +8, with the +9 and +10 generating significant fragmentation (data not shown). SI Figure 3 displays selected fragments following ETD for precursors from +7 to +10 and those produced from AI-ETD of the +7. AI-ETD of the +7 charge state leads to the formation of several product ions previously not observed, among them the $z^{\bullet}_3$, $z^{\bullet}_4$, c_5, and $z^{\bullet}_{17}{}^{+2}$ product ions. The $c_{17}{}^{+2}$ product ion (*m/z* = 961) is superposed with the $z^{\bullet}_{17}{}^{+2}$ product ion isotopic envelope for the +9 and +10 ubiquitin. This product ion was not observed for AI-ETD of the +7 charge state. The presence of these product ions demonstrates that IR photon bombardment of lower charge state cation precursors leads to protein unfolding, and ultimately gas phase conformations which resemble higher charge states.

Inspection of charge-reduced region:

Shown in Supporting Information Figure 4, panels A-E, is the *m/z* region occupied by the charge-reduction products of the precursor peptide having the sequence FSWGAEGQR for unassisted ETD and AI-ETD at 50, 75, and 99% laser power. Also shown is the theoretical proton transfer product isotope distribution, illustrated with the black dots. Inspection of the unassisted ETD charge-reduced region reveals that approximately 39% of the total ion current is due to ETnoD (estimated from product ion height). At 50, 75, and 99% laser power, this number drops to 28%, 15%, and 11% respectively.

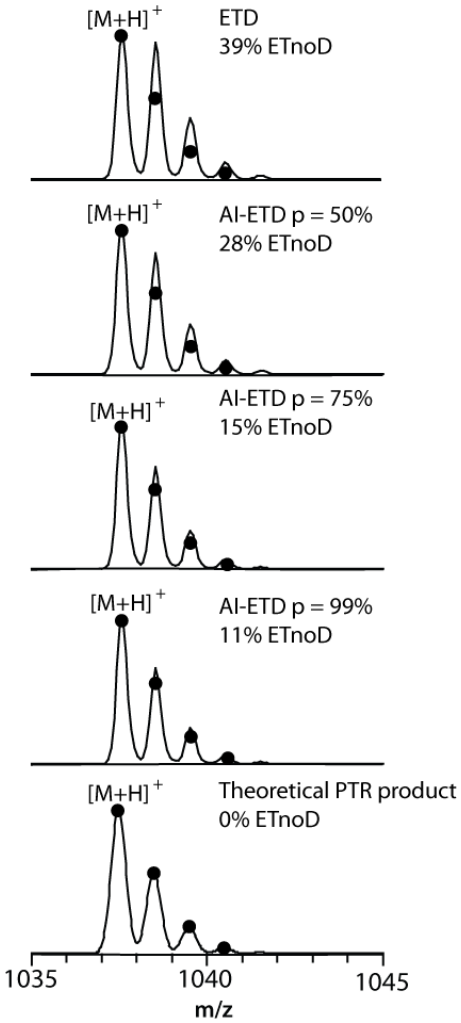

Supporting Information Figure 4. The charge-reduced *m/z* region of ETD (A). AI-ETD at 50, 75, and 99% laser power (B-D) and the theoretical proton-transfer product distribution (E) for peptide FSWGAEGQR. Non-theoretical products were generated *via* a 100 ms AI-ETD reaction at the laser power indicated.

Experimental Methods:

Materials: Peptides FSWGAEGQR and AGCKNFFWKTFTSC were purchased from BACHEM (Torrance, CA). All other chemicals unless otherwise indicated were purchase from from Sigma Aldrich (St. Louis, MO). Peptide solutions of ACTH (SYSHEMFRWGKPVGKKRRPVKVYP), Substance P (RPKPQQFFGLM), and Angiotensin (DRVYIHPFHL) were prepared by dissolving stock solutions to ~ 10pmol/µL in 70:29.9:0.1 acetonitrile/water/acetic acid by volume. Peptides solutions of FSWGAEGQR and AGCKNFFWKTFTSC were prepared by diluting stock solutions to a final concentration of ~ 10 pmol/ µL in 49:49:1 methanol/water/acetic acid by volume. Azobenzene was dissolved in toluene to a final concentration of ~ 1 mg/mL.

Instrumentation: All experiments were performed on a dual cell linear ion trap mass spectrometer consisting of a high pressure cell (HPC) and a low pressure cell (LPC) operated at 4.7 mTorr and 0.3 mTorr, respectively. 10.6 um irradiation from a model 48-5 Synrad 50 W CO_2 continuous wave laser (Mukilteo, WA) was introduced through a ZnSe window mounted to the back flange of the instrument on-axis with the dual cell trap as previously specified.[3] Instrument firmware was modified to externally trigger the laser concomitant with ion-ion reactions using pin 14 of the J1 connector on the digital printed circuit board. AI-ETD experiments were performed at full laser power unless otherwise specified.

Precursor cations and reagent anions were generated and infused into the mass spectrometer using a pulsed ESI-APCI scheme similar to that described by McLuckey et. al.[4] Briefly, the two sources were placed directly in front of the atmospheric inlet of the mass spectrometer. The ESI emitter tip position was optimized at a distance of ~ 35 mm from the inlet. Cations were introduced *via* direct infusion using a gastight syringe (Hamilton, Las Vegas, NV) at a rate of 1 µL/min. The ESI emitter tips used were 260 µm OD, 25 µm ID, with a 30 µm length (New Objective). The azobenzene solution was infused into the APCI probe (ThermoFisher Scientific, Bremen, Germany) at a rate of 1.5 µL/min. To prevent excessive adduction of oxygen with the radical azobenzene formed *via* APCI, the source region was aspirated with low purity nitrogen. For each scan, the ESI voltage was pulsed from 0 to 2.2 kV and the spray was allowed to stabilize for ~300 ms. Following accumulation of cations at

an AGC target of 10,000 precursor charges in the HPC, the electrospray voltage was switched back to zero and the corona pin voltage for the APCI source was pulsed from 0 to -5.5 kV and allowed to stabilize for ~400 ms. Anion injection and accumulation for ~10 ms immediately preceded ion-ion reactions. Following ion activation, the product ions were transferred to the LPC for *m/z* analysis. Note that bombardment of isolated radical anions of azobenzene with IR photons revealed neither dissociation nor electron detachment.

References

[1] C. Lin, J. J. Cournoyer, P. B. O'Connor, *J. Am. Soc. Mass Spectrom.* **2008**, *19*, 780.

[2] S. Myung, E. R. Badman, Y. J. Lee, D. E. Clemmer, J. Phys. Chem. A. **2002**, *106*, 9976.

[3] M. W. Gardner, L. A. Vasicek, S. Shabbir, E. V. Anslyn, J. S. Brodbelt, *Anal. Chem.*, **2008**, *80*, 4807

[4] X. Liang, Y. Xia, S. A. McLuckey, *Anal. Chem.* **2006**, *78*, 3208.